

Magnetization dependence on carrier doping in epitaxial ZnO thin films co-doped with Mn and P

M. Ivill and S. J. Pearton

Department of Materials Science and Engineering, University of Florida, Gainesville, Florida 32611-8440

Y. W. Heo

Department of Inorganic Materials Engineering, Kyungpook National University, Daegu, Korea

J. Kelly and A. F. Hebard

Department of Physics, University of Florida, Gainesville, Florida 32611-8440

D. P. Norton^{a)}

Department of Materials Science and Engineering, University of Florida, Gainesville, Florida 32611-8440

(Received 23 July 2006; accepted 10 April 2007; published online 21 June 2007)

The magnetic and transport properties of Mn-doped ZnO thin films co-doped with P are examined. Superconducting quantum interference device magnetometry measurements indicate that the films are ferromagnetic with an inverse correlation between magnetization and electron density as controlled by P doping. In particular, under conditions where the acceptor dopants are activated leading to a decrease in free-electron density, magnetization is enhanced. The result is consistent with hole-mediated ferromagnetism in Mn-doped ZnO, in which bound acceptors mediate the ferromagnetic ordering. Increasing the electron density decreases the acceptor concentration, thus quenching the ferromagnetic exchange. This result is important in understanding ferromagnetism in transition metal doped semiconductors for spintronic devices. © 2007 American Institute of Physics. [DOI: 10.1063/1.2739302]

I. INTRODUCTION

Spintronics with magnetically doped semiconductors has the potential to provide enhanced performance and new functionality in semiconducting devices, including spin-based field-effect transistors (FETs), spin-polarized lasers and light emitting diodes (LEDs), nonvolatile magnetic semiconductor memory, and perhaps quantum computing.^{1,2} Research in dilute magnetic semiconductors (DMS)³⁻⁷ has been stimulated by the discovery of materials with a Curie temperature, T_c , significantly higher than that observed in previously studied DMS materials. In particular, the experimental T_c for Mn-doped GaAs is on the order of 110 K.⁸ However, the penetration of spintronics as a technology depends upon the development and understanding of semiconductors that can support spin-polarized carrier operation at or above room temperature.

Several magnetically doped semiconductors have recently been discovered that exhibit ferromagnetic ordering above room temperature,⁹⁻¹² including transition metal doped ZnO. ZnO is a direct wide band-gap material of interest for photonic, electronic, and magnetic applications.^{13,14} Ferromagnetism was initially predicted by Dietl *et al.* in *p*-type Mn-doped ZnO.¹⁵ Zener's model was used as the basis, driven by exchange interaction between hole charge carriers and localized spins. Numerous studies have since addressed the magnetic properties of transition metal doped ZnO, with most activities focusing on cobalt or manganese doping.¹⁶⁻³³ For Mn-doped ZnO, Jung *et al.*²¹ reported low

T_c (45 K) ferromagnetism, whereas Fukumura *et al.*²² observed spin-glass behavior with a spin-freezing temperature of 13 K. For Mn doping, we have reported ferromagnetism with a Curie temperature approaching 250 K in Mn, Sn-doped ZnO.^{23,24} High-temperature ferromagnetism was also reported in (Zn,Mn)O by Sharma *et al.*, with a T_c above 425 K in bulk crystals and above 300 K in thin films.¹² Mn-doped ZnO, with an apparent T_c above 300 K, appears attractive for spintronic technology. With a lack of high-temperature ferromagnetic secondary phases in the Zn-Mn-O phase diagram, this material is particularly useful in delineating the origin of ferromagnetism in a semiconductor host. The only ferromagnetic composition for this solid solution is Mn₃O₄, which is ferrimagnetic with a Curie temperature of less than 50 K.^{34,35} Therefore, any room-temperature ferromagnetism cannot be assigned to known secondary phases as none exist. The possible presence of secondary ferromagnetic phases cannot be easily eliminated as the origin of the magnetic signals for other transition metal dopants.

Despite experiments indicating high-temperature ferromagnetism in these materials, questions remain regarding the origin of the magnetic behavior in Mn-doped ZnO materials. Dietl's work predicted that highly *p*-type, Mn-doped ZnO should have Curie temperatures in excess of room temperature.^{15,36,37} The theory assumes that ferromagnetic ordering between the localized moments of the Mn atoms is mediated by free holes in the material. High hole concentrations should yield high Curie temperatures; carrier-mediated ferromagnetism in *n*-type material should be limited to lower temperatures. This distinction in carrier type is attributed to the smaller density of states and exchange integral for Mn

^{a)}Author to whom correspondence should be addressed; FAX: 352-846-1182; electronic mail: dnort@mse.ufl.edu

with the conduction band in comparison to the valence band,³⁸ as the Mn^{2+} state lies within the valence band of these materials. For wide band-gap semiconductors, the exchange interaction for Mn is fundamentally different from the other transition metal ions. Mn d states lie in the valence band while the other transition metals d -state orbitals introduce states within the gap. There are also apparent discrepancies between experimental results and Dietl's model for Mn-doped ZnO. In some materials, ferromagnetism has been reported in n -type and/or semi-insulating samples. Formation of p -type ZnO with high carrier density is a significant challenge that is being actively pursued for electronic applications.³⁹ An alternative model addresses whether ferromagnetic ordering of the Mn moments could originate from carriers (holes) that are present in the material, but localized at the transition metal impurity.^{40,41} The bound magnetic polaron model assumes an exchange interaction between the transition metal (Mn) ion and localized (trapped) holes that are spatially near the Mn ion. The size of the bound magnetic polaron grows as temperature decreases until its radius overlaps that of neighboring polarons. This enables ferromagnetic ordering of the Mn ions in an otherwise insulating or semi-insulating material. Ferromagnetic ordering appears possible with a bound magnetic polaron model. However, for Mn, it still depends on the availability of holes, albeit a localized distribution.

In this paper, we report on the synthesis and magnetic properties of Mn-doped ZnO epitaxial films that are co-doped with P. Co-doping allows independent control over the magnetic and electronic properties of the material by doping for each separately. In II-VI materials, the addition of Mn^{2+} does not introduce shallow states. By co-doping II-VI semiconductors, Mn provides the localized spins needed for carrier-mediated ferromagnetism, with the additional dopant added to control the carrier concentration in the material. We investigated the carrier density dependence of saturation magnetization, using P as an acceptor dopant.

II. EXPERIMENTS

Epitaxial Mn, P-doped ZnO films were grown by conventional pulsed-laser deposition. Laser ablation targets were prepared from high purity powders of ZnO (99.999%), with MnO_2 (99.999%) and P_2O_5 (99.95%) serving as the doping agents. The pressed targets were sintered at 1000 °C for 12 h in air. The targets were fabricated with a nominal composition of 3 at. % Mn and 2 at. % P. A Lambda Physik KrF excimer laser was used as the ablation source. The laser energy density was 1–3 J/cm² with a laser repetition rate of 1 Hz and target-to-substrate distance of 6 cm. The growth chamber exhibits a base pressure of 10⁻⁵ Torr. Films were deposited onto single-crystal, c -plane-oriented sapphire substrates. Film growth was conducted over a temperature range of 400–600 °C. An oxygen pressure of 20 mTorr was used for all film growth experiments. Film thicknesses were approximately 300–400 nm. X-ray diffraction was used to determine the crystallinity and secondary phase formation. Su-

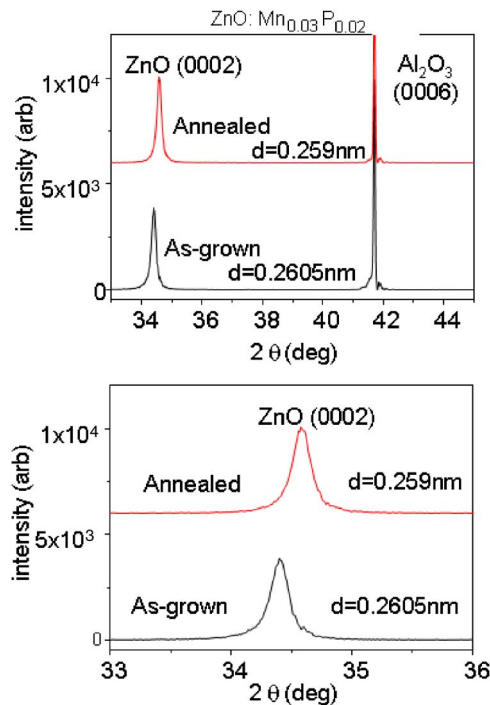


FIG. 1. X-ray diffraction of ZnO films co-doped with Mn and P both before and after annealing. The target was ZnO doped with 3%Mn and 2%P.

perconducting quantum interference device (SQUID) magnetometry was used to characterize the ferromagnetic behavior of the doped films.

III. RESULTS

The phase stability and solid solubility of Mn in the ZnO films were investigated before and after annealing for films with P co-doping. Figure 1 shows the x-ray diffraction scans for films deposited under the given growth conditions. In all cases, the dominant film peaks correspond to c -axis perpendicular ZnO. Note that, for these films, segregation of the Mn_3O_4 phase is not observed in the diffraction data. As mentioned earlier, the Mn_3O_4 phase is ferromagnetic with a Curie temperature of less than 50 K. Previous reports from Fukumura *et al.* indicated that epitaxial ZnO films with a Mn concentration as high as 35% could be achieved while maintaining the wurtzite structure using pulsed laser deposition.⁴² Upon annealing, a shift in the d -spacing for the ZnO is observed. This may indicate a segregation of either P or Mn in the films with thermal processing.

Defect chemistry calculations for Mn-doped ZnO indicate that Mn^{2+} forms a donor level ~ 2.0 eV below the conduction band edge.⁴³ This deep donor level with Mn substitution on the Zn site in ZnO has no direct effect on the electron concentration at room temperature. However, defect chemistry calculations also indicate a reduction in Zn interstitials with Mn doping. Zn interstitials are generally accepted as the primary shallow donor defects in nominally undoped ZnO. This will yield an increase in resistivity for Mn-doped films as compared to undoped material.^{43–45} The Mn-doped ZnO films with no P exhibit a resistivity on the order of 10² Ω cm with a carrier density of mid-10¹⁶/cm³. This carrier density is substantially lower than that seen for

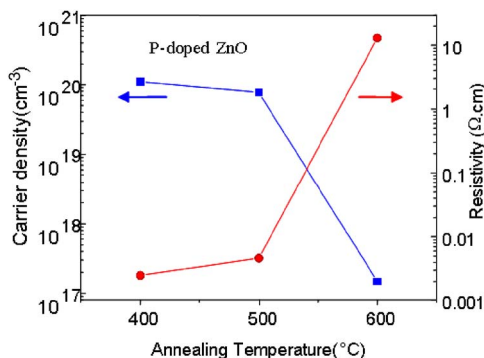


FIG. 2. Resistivity and carrier concentration behavior of P-doped ZnO films both as deposited and annealed in oxygen. The data shown is for 1 at. % P-doped ZnO.

undoped epitaxial films and is consistent with the reduction of shallow donors. Limited results on the doping behavior of P in ZnO indicate that it introduces a donor state for as-deposited films, an acceptor state when annealed.

The behavior of phosphorus in ZnO epitaxial films both as deposited and upon annealing has been reported in detail elsewhere.⁴⁶ For the as-deposited films, the inclusion of phosphorus yields a significant increase in electron density, resulting in ZnO that is highly conductive and *n* type. The shallow donor behavior in the as-deposited films is inconsistent with P substitution on the O site, and presumably originates from either substitution on the Zn site or the formation of a phosphorus-bearing complex. Previous work has shown that the defect-related carrier density in nominally undoped ZnO can be reduced via high-temperature annealing in oxygen or air. In the case of undoped material, the reduction in donor density is presumed due to either a reduction in oxygen vacancies, Zn interstitials, or perhaps out diffusion of hydrogen that is incorporated in the ZnO lattice during synthesis. In order to reduce electron density annealing in oxygen can be performed. Figure 2 shows the resistivity of films annealed at various temperatures. Note that the resistivity of the as-deposited phosphorus-doped films is significantly lower than that for the nominally undoped film. For as-deposited films, a shallow donor state dominates transport. As the films are annealed at increasing temperatures, the resistivity of the phosphorus-doped films increases rapidly. This is particularly evident for films subjected to annealing temperatures of 600 °C or higher. When annealed at 700 °C, the phosphorus-doped ZnO films become semi-insulating with a resistivity approaching 10⁴ Ω cm. The conversion of transport behavior from highly conducting to semi-insulating with annealing should be attributed to at least two factors. First, the defect associated with the shallow donor state in as-deposited films appears to be relatively unstable. This would explain the increase in resistivity, but would alone predict a saturation of resistivity at the value given by the undoped material. The dependence of postannealed resistivity on phosphorus content suggests that a deep level associated with phosphorus dopant is present. This is, in fact, consistent with the expected results that P substitution on the oxygen site yields a deep acceptor. Figure 2 also shows the carrier concentration for P-doped films. For all of the data

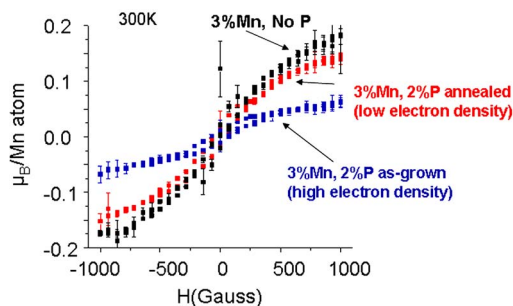


FIG. 3. Room-temperature SQUID measurements for epitaxial ZnO:3%Mn, 2%P films before and after anneal. Also shown is a ZnO:Mn film with no P.

shown in Fig. 2, the Hall sign was negative, indicating *n*-type material. Both carrier density and Hall mobility data for some annealed samples are absent in the plots. From the measurements yielding unambiguous Hall voltage, both the carrier density and mobility in phosphorus-doped films are observed to decrease with annealing. This is consistent with a reduction in the shallow donor state density and activation of a deep (acceptor) level in the gap.

The magnetic properties of the films were measured using a Quantum Design SQUID magnetometer. The diamagnetic responses of the substrate and host semiconductor were subtracted from the magnetization plots. The primary focus of the measurements was to determine how the magnetic properties of the films changed as a function of electron density as controlled by P doping. Samples that showed minimal amounts of Mn₃O₄ precipitation via x-ray diffraction were used for the SQUID measurements. Figure 3 shows the room-temperature magnetization as a function of applied magnetic field for epitaxial ZnO:3%Mn films both without and with P co-doping. For the Mn-doped film with no P, saturation in the magnetization is observed, but with little evidence for hysteresis in the M versus H curves. The as-deposited ZnO film doped with both Mn and P showed a reduction in magnetization/Mn ion. This is consistent with the proposed models for Mn-doped ZnO, where ferromagnetic ordering is not favored by electron doping. Most interesting is the saturation magnetization behavior as the P-doped samples are annealed. As noted earlier, increasing P concentration in as-deposited films initially increases electron density and conductivity. Figure 3 shows the room-temperature magnetization versus field behavior for the ZnO samples containing 3%Mn and 2 at. % P annealed in oxygen. Magnetization is given as the magnetic moment/Mn dopant ion. Initially, there is a decrease in magnetization with P doping. However, with annealing, there is an inverse correlation between the electron carrier concentration and saturation magnetization. Similar results are seen at 10 K as shown in Fig. 4. Initially, as the electron density increases with P doping, the magnetization decreases. This is consistent with the bound magnetic polaron model in which only a fraction of the Mn ions are expected to order ferromagnetically due to competing superexchange antiferromagnetic interactions between neighboring Mn ions.⁴⁷ The inverse correlation of saturation magnetization with electron density is interesting and provides some insight into the mechanism for ferromagnetism in Mn-doped ZnO. Overlap of the Mn *d* states with

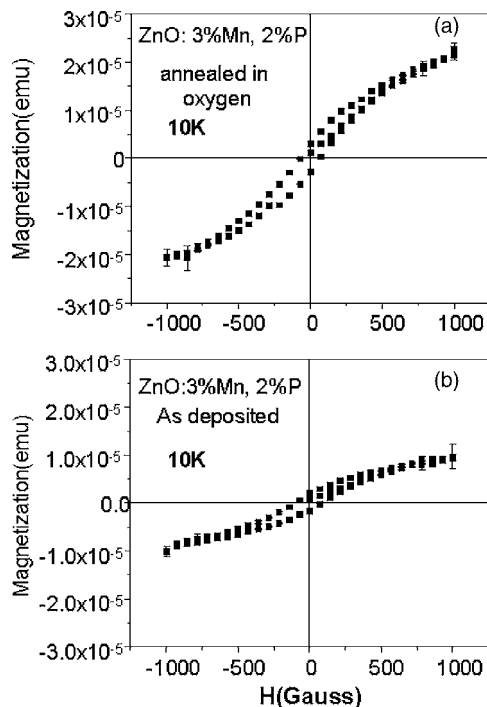


FIG. 4. SQUID measurements at 10 K for epitaxial ZnO:3%Mn, 2%P films (a) after annealing and (b) before annealing.

the valence band suggests that holes are necessary in order to induce ferromagnetic order. For semi-insulating films to exhibit ferromagnetism, the bound magnetic polaron model provides a mechanism whereby holes that are localized at or near the Mn ions are responsible for mediating ferromagnetism. However, the most important observation is that the activation of acceptor states for hole formation is necessary in order to achieve ferromagnetism. The holes may be delocalized, but with low mobility, thus yielding low conductivity. In this case, the carrier-mediated mechanism may suffice without the need of invoking bound polarons as inherent to the ferromagnetic ordering. In either case, the addition of electrons to the system will move the Fermi energy level up in the band gap, resulting in a decrease in hole density and a reduction in magnetization. Our results are consistent with those reported on a similar set of experiments involving ZnO:Mn co-doped with phosphorus.⁴⁸ This appears consistent with early work on trivalent doped (Zn,Mn)O, where no ferromagnetism was observed for heavily *n*-type films. It may also explain the discrepancy from other studies of Mn-doped ZnO films in which the intrinsic defect-mediated donor states are high in density. It should be noted that the amount of magnetization in the material remains relatively low at all temperatures as seen in the temperature-dependent magnetization data in Fig. 5. It is important to note the need to maintain a Mn concentration low enough to avoid Mn-Mn antiferromagnetic interactions, which are likely to dominate high-Mn-doped ZnO films.

The results of this study are consistent with previous studies on the carrier-type dependence in Co- and Mn-doped ZnO nanocrystalline films.^{49,50} In that case, ferromagnetism was observed in Mn-doped ZnO nanocrystals only when nitrogen, a group V acceptor dopant, was introduced during the

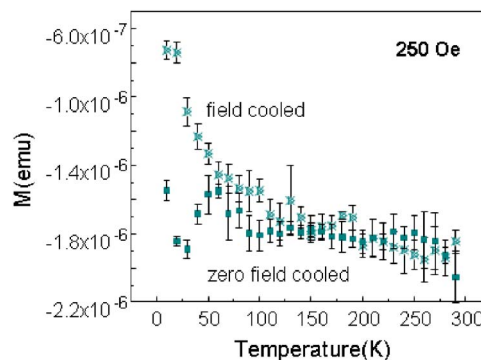


FIG. 5. Field-cooled and zero-field-cooled magnetization measurements for annealed film.

synthesis process. In contrast, no ferromagnetism was observed in Co-doped ZnO nanocrystals when processed with nitrogen. Based on this and other properties, the authors conclude that ferromagnetism in ZnO is closely tied to the charge transfer electronic structure of the transition metal dopant. For Mn, ferromagnetism is induced when the holes from the acceptor ion delocalize onto Mn²⁺. Again, our results are consistent with this conclusion.

ACKNOWLEDGMENTS

The work at UF is partially supported by the Air Force Office of Scientific Research (AFOSR) under Grant No. 4559-005; the Army Research Office under Grant No. DAAD19-01-1-0603; NSF Grant No. CTS-0301178 monitored by Dr. M. Burka and Dr. D. Senich; by NASA Kennedy Space Center Grant No. NAG 10-316 monitored by Daniel E. Fitch; and the National Science Foundation Grants Nos. DMR 0400416 and 0101856. The authors would like to acknowledge the Major Analytical Instrumentation Center, Department of Materials Science and Engineering, University of Florida.

¹S. A. Wolf, D. D. Awschalom, R. A. Buhrman, J. M. Daughton, S. von Molnár, M. L. Roukes, A. Y. Chtchelkanova, and D. M. Treger, *Science* **294**, 1488 (2001).

²G. A. Prinz, *Science* **282**, 1660 (1998).

³J. K. Furdyna, *J. Appl. Phys.* **64**, R29 (1988).

⁴S. Gopalan and M. G. Cottam, *Phys. Rev. B* **42**, 10311 (1990).

⁵C. Haas, *CRC Crit. Rev. Solid State Sci.* **1**, 47 (1970).

⁶T. Suski, J. Igalson, and T. Story, *J. Magn. Magn. Mater.* **66**, 325 (1987).

⁷A. Haury, A. Wasiela, A. Arnoult, J. Cibert, S. Tatarenko, T. Dietl, and Y. Merle d'Aubigne, *Phys. Rev. Lett.* **79**, 511 (1997); P. Kossacki, D. Ferrand, A. Arnoult, J. Cibert, S. Tatarenko, A. Wasiela, Y. Merle d'Aubigne, J.-L. Staihl, J.-D. Ganiere, W. Bardyszewski, K. Swiatek, M. Sawicki, J. Wrobel, and T. Dietl, *Physica E (Amsterdam)* **6**, 709 (2000).

⁸H. Ohno, *Science* **281**, 951 (1998).

⁹S. J. Pearton, C. R. Abernathy, D. P. Norton, A. F. Hebard, Y. D. Park, L. A. Boatner, and J. D. Budai, *Mater. Sci. Eng., R.* **40**, 137 (2003).

¹⁰M. Ivill, M. E. Overberg, C. R. Abernathy, D. P. Norton, A. F. Hebard, N. Theodoropoulou, and J. D. Budai, *Solid-State Electron.* **47**, 2215 (2003).

¹¹Y. Matsumoto, M. Murakami, T. Shono, T. Hasegawa, T. Fukumura, M. Kawasaki, P. Ahmet, T. Chikyow, K. Shin-ya, and H. Koinuma, *Science* **291**, 854 (2001).

¹²P. Sharma, A. Gupta, K. V. Rao, F. J. Owens, R. Sharma, R. Ahuja, J. M. Osorio Guillen, B. Johansson, and G. A. Gehring, *Nat. Mater.* **2**, 673 (2003).

¹³D. C. Look, *Mater. Sci. Eng. B* **80**, 383 (2001).

¹⁴S. Masuda, K. Kitamura, Y. Okumura, S. Miyatake, H. Tabata, and T. Kawai, *J. Appl. Phys.* **93**, 1624 (2003).

- ¹⁵T. Dietl, H. Ohno, F. Matsukura, J. Cubert, and D. Ferrand, *Science* **287**, 1019 (2000).
- ¹⁶K. Sato and H. Katayama-Yoshida, *Jpn. J. Appl. Phys., Part 2* **39**, L555 (2000).
- ¹⁷J. H. Kim, H. Kim, D. Kim, Y. E. Ihm, and W. K. Choo, *J. Appl. Phys.* **92**, 6066 (2002).
- ¹⁸H.-J. Lee, S.-Y. Jeong, C. R. Cho, and C. H. Park, *Appl. Phys. Lett.* **81**, 4020 (2002).
- ¹⁹T. Wakano, N. Fujimura, Y. Morinaga, N. Abe, A. Ashida, and T. Ito, *Physica E (Amsterdam)* **10**, 260 (2001).
- ²⁰S.-J. Han, J. W. Song, C.-H. Yang, S. H. Park, J.-H. Park, Y. H. Jeong, and K. W. Rhie, *Appl. Phys. Lett.* **81**, 4212 (2002).
- ²¹S. W. Jung, S.-J. An, G.-C. Yi, C. U. Jung, S.-I. Lee, and S. Cho, *Appl. Phys. Lett.* **80**, 4561 (2002).
- ²²T. Fukumura, Z. Jin, M. Kawasaki, T. Shono, T. Hasegawa, S. Koshihara, and H. Koinuma, *Appl. Phys. Lett.* **78**, 958 (2001).
- ²³D. P. Norton, S. J. Pearton, A. F. Hebard, N. Theodoropoulou, L. A. Boatner, and R. G. Wilson, *Appl. Phys. Lett.* **82**, 239 (2003).
- ²⁴M. Ivill, S. J. Pearton, D. P. Norton, J. Kelly, and A. F. Hebard, *J. Appl. Phys.* **97**, 053904 (2005).
- ²⁵Y. Q. Chang, D. B. Wang, X. H. Luo, X. Y. Xu, X. H. Chen, L. Li, C. P. Chen, R. M. Wang, J. Xu, and D. P. Yu, *Appl. Phys. Lett.* **83**, 4020 (2003).
- ²⁶A. S. Risbud, N. A. Spaldin, Z. Q. Chen, S. Stemmer, and R. Seshadri, *Phys. Rev. B* **68**, 205202 (2003).
- ²⁷S.-J. Han, T.-H. Jang, Y. B. Kim, B.-G. Park, J.-H. Park, and Y. H. Jeong, *Appl. Phys. Lett.* **83**, 920 (2003).
- ²⁸S. W. Yoon, S.-B. Cho, S. C. We, S. Yoon, B. J. Suh, H. K. Song, and Y. J. Shin, *J. Appl. Phys.* **93**, 7879 (2003).
- ²⁹V. A. L. Roy, A. B. Djurisic, H. Liu, X. X. Zhang, Y. H. Leung, M. H. Xie, J. Gao, H. F. Lui, and C. Surya, *Appl. Phys. Lett.* **84**, 756 (2004).
- ³⁰X. M. Cheng and C. L. Chien, *J. Appl. Phys.* **93**, 7876 (2003).
- ³¹S. S. Kim, J. H. Moon, B.-T. Lee, O. S. Song, and J. H. Je, *J. Appl. Phys.* **95**, 454 (2004).
- ³²S. Kolesnik, B. Dabrowski, and J. Mais, *J. Appl. Phys.* **95**, 2582 (2004).
- ³³J. Zhang, R. Skomski, and D. J. Sellmyer, *J. Appl. Phys.* **97**, 10D303 (2005).
- ³⁴L. W. Guo, D. L. Peng, H. Makino, K. Inaba, H. J. Ko, K. Sumiyama, and Y. Yao, *J. Magn. Magn. Mater.* **213**, 321 (2000).
- ³⁵A. Chartier, P. D'Arco, R. Dovesi, and V. R. Saunders, *Phys. Rev. B* **60**, 14042 (1999).
- ³⁶T. Dietl, A. Hauray, and Y. Merle d'Aubigne, *Phys. Rev. B* **55**, R3347 (1997).
- ³⁷T. Dietl, *Semicond. Sci. Technol.* **17**, 377 (2002).
- ³⁸H. Ohno, *Semiconductor Spintronics and Quantum Computation*, edited by D. D. Awschalom, D. Loss, and N. Samarth (Springer, New York, 2002), Chap. 1.
- ³⁹D. C. Look, D. C. Reynolds, C. W. Litton, R. L. Jones, D. B. Eason, and G. Cantwell, *Appl. Phys. Lett.* **81**, 1830 (2002).
- ⁴⁰A. Kaminski and S. Das Sarma, *Phys. Rev. Lett.* **88**, 247202 (2002).
- ⁴¹M. Berciu and R. N. Bhatt, *Phys. Rev. Lett.* **87**, 107203 (2001).
- ⁴²T. Fukumura, Z. Jin, A. Ohtomo, H. Koinuma, and M. Kawasaki, *Appl. Phys. Lett.* **75**, 3366 (1999).
- ⁴³J. Han, P. Q. Mantas, and A. M. R. Senos, *J. Eur. Ceram. Soc.* **22**, 49 (2002).
- ⁴⁴Z. Zhou, K. Kato, T. Komaki, M. Yoshino, H. Yukawa, M. Morinaga, and K. Morita, *J. Eur. Ceram. Soc.* **24**, 139 (2004).
- ⁴⁵N. Ohashi, J. Tanaka, T. Ohgaki, H. Haneda, M. Ozawa, and T. Tsurumi, *J. Mater. Res.* **17**, 1529 (2002).
- ⁴⁶Y. W. Heo, Y. W. Kwon, Y. Li, S. J. Pearton, and D. P. Norton, *J. Electron. Mater.* **34**, 409 (2005).
- ⁴⁷T. Dietl, M. Sawicki, L. Van Khoi, J. Jaroszyński, P. Kossacki, J. Cibert, D. Ferrand, S. Tatarenko, and A. Wasiela, *Phys. Status Solidi B* **229**, 665 (2002).
- ⁴⁸Q. Wan, *Appl. Phys. Lett.* **89**, 082515 (2006).
- ⁴⁹K. R. Kittilstved, W. K. Liu, and D. R. Gamelin, *Nat. Mater.* **5**, 291 (2006).
- ⁵⁰K. R. Kittilstved, N. S. Norberg, and D. R. Gamelin, *Phys. Rev. Lett.* **94**, 147209 (2005).